Wound Healing

Authors: **Raul Adell Segarra, Vicent Navarro Arroyo, Roger Pascual Mellado**

Subject: Computational Mechanics

2023

Facultat de Matemàtiques i Estadística
Master in Advanced Mathematics and Mathematical Engineering

1 Theoretical background

1.1 Question 1

The Figure (1) replicates the figure shown in the referenced article, in which four configurations are designed to emulate distinct states of dermal tissue.

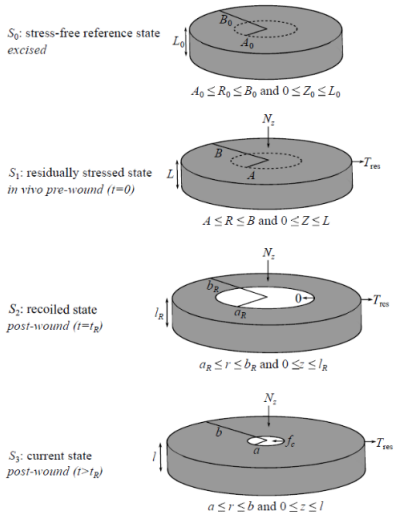

Figure 1: Schematic representation of the mathematical model.

- *Configuration* S_0: It represents a stress-free state of non-wounded tissue. An example of such a state could be the tissue surrounding the knee when the leg is fully extended.
- *Configuration* S_1: It represents a stressed state of non-wounded tissue. Continuing with the previous analogy, it could represent the same knee tissue, but when the leg is flexed.
- *Configuration* S_2: It represents wounded tissue before the healing process, where the wound occurs on a tissue section subjected to the residual stress of configuration S_2. The tissue recoils in order to release the previously stored elastic energy.
- *Configuration* S_3: It corresponds to a wounded tissue in the healing stage. In this configuration, the tissue is attempting to recover from the previously described recoiling and initiates the healing process.

Now we will discuss how equation (4) of the mentioned article is derived. To begin, the geometric deformation tensor is introduced, and it is explicitly defined as follows:

$$\mathbf{F} = diag\left(\frac{\partial r}{\partial R_0}, \frac{r}{R_0}, \lambda\right).$$

Moreover, this tensor can be written as $\mathbf{F} = \mathbf{A} \cdot \mathbf{G}$, where $\mathbf{A}$ is an elastic contribution and $\mathbf{G}$ is a growth contribution and

$$\mathbf{G} = \text{diag}(\gamma_r, \gamma_\theta, \gamma_z), \quad \mathbf{A} = \text{diag}(\alpha_r, \alpha_\theta, \alpha_z).$$

The skin is assumed to be almost incompressible, so $\det(\mathbf{A}) = 1$. Therefore, we obtain

$$\frac{\partial r}{\partial R_0} \cdot \frac{r}{R_0} \cdot \lambda = \det(\mathbf{F}) = \det(\mathbf{A}) \cdot \det(\mathbf{G}) = \det(\mathbf{G}) = \gamma_r \gamma_\theta \gamma_z,$$

which can be rewritten as equation (3) in the article:

$$\frac{r}{R_0} = \frac{\gamma_r \gamma_\theta \gamma_z R_0}{\lambda r},$$

which is an ODE that can be solved using separation of variables as

$$\frac{r^2(R_0) - r^2(A_0)}{2} = \int_{A_0}^{R_0} r \, \partial r = \int_{A_0}^{R_0} \frac{\gamma_r \gamma_\theta \gamma_z \tilde{R}}{\lambda} \, \partial \tilde{R}$$

Using the boundary condition $r^2(A_0) = a^2$ and making the dependency of γ with respect to $\tilde{R}$ explicit, we finally obtain the desired equation as:

$$r^2(R_0) = a^2 + 2 \int_{A_0}^{R_0} \frac{\gamma_r(\tilde{R}) \gamma_\theta(\tilde{R}) \gamma_z(\tilde{R}) \tilde{R}}{\lambda} \, \partial \tilde{R}. \tag{1}$$

It will be beneficial for future reference to observe that once the function r is specified, we can retrieve the elements of the elastic tensor by considering that

$$\boldsymbol{F} = \operatorname{diag}\left(\frac{\partial r}{\partial R_0}, \frac{r}{R_0}, \lambda\right) = \boldsymbol{A} \cdot \boldsymbol{G} = \operatorname{diag}\left(\alpha_r \gamma_r, \alpha_\theta \gamma_\theta, \alpha_z \gamma_z\right)$$

i.e.,

$$\begin{cases} \alpha_r = \dfrac{\partial r}{R_0} \dfrac{1}{\gamma_r} = \dfrac{\gamma_\theta \gamma_z}{r \lambda} R_0 \\ \alpha_\theta = \dfrac{r}{\gamma_\theta R_0} \\ \alpha_z = \dfrac{\lambda}{\gamma_z} \end{cases} \tag{2}$$

1.2 Question 2

Let us present and explain the different hypotheses that are used in the wound-healing model.

1. **The fundamental assumption of morphoelasticity**. The deformation is conceptualized as a composite of two distinct processes, as discussed earlier. We express this deformation as $F = A \cdot G$, where the growth tensor G characterizes the incorporation or removal of material within the body, while the elastic tensor A captures the resultant elastic deformation.

2. **Symmetric deformations**. In cylindrical coordinates, the off-diagonal strains related to the displacement vector $u = (u_r; u_\theta; u_z)$ (note that this notation differs from that used in the article) can be expressed as:

$$\varepsilon_{r\theta} = \frac{1}{2}\left(\frac{1}{r}\frac{\partial u_r}{\partial \theta} + \frac{\partial u_\theta}{\partial r} - \frac{u_\theta}{r}\right), \quad \varepsilon_{\theta z} = \frac{1}{2}\left(\frac{\partial u_\theta}{\partial z} + \frac{1}{r}\frac{\partial u_z}{\partial \theta}\right), \quad \varepsilon_{zr} = \frac{1}{2}\left(\frac{\partial u_r}{\partial z} + \frac{\partial u_z}{\partial r}\right).$$

   Due to the presence of axial and azimuthal symmetry in the problem, we have $\partial/\partial z = 0$ and $\partial/\partial \theta = 0$, resulting in the following expressions: The expressions in cylindrical coordinates for the strain components

are as follows:

$$\varepsilon_{r\theta} = \frac{1}{2}\left(\frac{\partial u_\theta}{\partial r} - \frac{u_\theta}{r}\right), \quad \varepsilon_{\theta z} = 0, \quad \varepsilon_{zr} = \frac{1}{2}\frac{\partial u_z}{\partial r}$$

Additionally, considering the absence of torque effects and the assumption of specimen homogeneity, we expect u_θ to be zero, leading to the vanishing of the $\varepsilon_{r\theta}$ term. Furthermore, while u_z may not be zero, its derivative with respect to r is expected to be zero due to the homogeneity assumption.

3. **Skin incompressibility**. This hypothesis is derived from experimental observations, as stated in the article. It is based on the principle that an infinitesimal element of the skin must maintain its volume, which mathematically implies that $\det(\mathbf{A}) = 1$, where $\mathbf{A}$ represents the elastic tensor.

4. **Neo-Hookean material model for dermal tissue**. This model is well-suited for describing hyperelastic materials, as it can accurately predict the nonlinear stress-strain behavior of materials experiencing significant deformations. It achieves this by introducing an alternative definition of the strain energy density function. This modified definition ensures that the resulting stress-strain curve exhibits an initial linear region, followed by a plateau phase.

5. **No body forces**. There are no volumetric external forces acting on the specimen.

6. **Mechanical equilibrium is reached after $\mathbf{F}_1$ and $\mathbf{F}_2$ deformations**. In simpler terms, the model assumes that the transient state, or any dynamic effects, can be neglected. This is known as the quasi-static hypothesis, where the focus is primarily on the behavior of the material under static or slowly changing conditions.

7. **Plane stress**. In this context, it is assumed that there are no forces acting specifically along the axial direction. However, it is acknowledged that deformation can still occur in that direction. This means that while there may be axial deformation, it is not directly caused by any applied forces along that axis.

8. **The residual tension of state S_1 is due to pressure at the external boundary**. Indeed, it is stated as an assumption that there are no body forces acting in the system. However, it should be noted that after this assumption is made, the residual tension of S_1 can only be present if an external force, represented by T_{res}, is applied at the boundary. In other words, the residual tension in S_1 arises solely due to the application of this external force at the boundary.

1.3 Question 3

The tensor $\mathbf{F}_1$ describes the deformation between the initial state, denoted as S_0, and the state S_1 as illustrated in Figure (1). This deformation is solely caused by the external tension T_{res} applied to the boundary, representing the prewound state.

Upon the occurrence of winding, a discontinuous jump leads to the recoiled state, characterized by the presence of a cylindrical hole and the same external tension T_{res} at the boundary as in state S_1. This recoiled state is described by the tensor $\mathbf{F}_2$, which is defined as:

$$\mathbf{F}_2 = \frac{\partial \mathbf{x}_R}{\partial \mathbf{X}_0}$$

This tensor relates the deformation in the recoiled state to the initial condition at S_0.

1.4 Question 4

To address this requirement, let's start by introducing the mechanical system of equations that governs the model.
On the one hand, we impose the balance of momentum (both linear and angular), which leads to:

$$\rho\ddot{x} = \nabla \cdot \mathbf{T} + \rho\mathbf{f}_b,$$

Here, ρ represents the density of the tissue, $\mathbf{f}_b$ denotes an external body force, and $\mathbf{T}$ is the Cauchy stress tensor, which is symmetric due to the balance of angular momentum. Additionally, based on the hypothesis stated in the second requirement, we assume that the stress tensor is diagonal, i.e., $\mathbf{T} = \text{diag}(T_{rr}, T_{\theta\theta}, T_{zz})$. We also consider the assumption of a plane stress framework, which implies that $T_{rr} = 0$. Furthermore, equilibrium is achieved after both deformations. Thus, the balance of momentum equation without body forces simplifies to:

$$\nabla \cdot \mathbf{T} = 0.$$

In cylindrical coordinates and for this particular case, the equation simplifies to:

$$(0,0,0) = \nabla \cdot \mathbf{T} = \left(\frac{\partial T_{rr}}{\partial r} + \frac{1}{r}(T_{rr} - T_{\theta\theta}), \frac{1}{r}\frac{\partial T_{\theta\theta}}{\partial \theta}, 0 \right),$$

The unique non-trivial component of the equation can be expressed as:

$$\frac{\partial T_{rr}}{\partial r} + \frac{1}{r}(T_{rr} - T_{\theta\theta}) = 0. \tag{3}$$

On the other hand, let's consider the stress-strain constitutive relation provided by the Neo-Hookean material model, which is given by:

$$\mathbf{T} = \mathbf{A} \cdot \frac{\partial W}{\partial \mathbf{A}} - p\mathbf{I}.$$

In the given equation, the function $W = W(\alpha_r; \alpha_\theta; \alpha_z)$ represents a specific strain energy function employed in this model. In our particular case, we adopt the following form for W:

$$W(\alpha_r; \alpha_\theta; \alpha_z) = \frac{\mu}{2}(\alpha_r^2 + \alpha_\theta^2 + \alpha_z^2 - 3),$$

where μ corresponds to the tissue stiffness. Note that when the material is at rest the energy strain function, W, will be zero because $\alpha_r = \alpha_\theta = \alpha_z = 1$.
By substituting this strain energy definition into the constitutive law, we obtain the following relationships:

$$T_{rr} = \alpha_r \frac{\partial W}{\partial \alpha_r} - p = \mu\alpha_r^2 - p, \;\; T_{\theta\theta} = \alpha_\theta \frac{\partial W}{\partial \alpha_\theta} - p = \mu\alpha_\theta^2 - p, \;\; T_{zz} = \alpha_z \frac{\partial W}{\partial \alpha_z} - p = \mu\alpha_z^2 - p. \tag{4}$$

It is important to note that the assumption of plane stress results in $p = \mu\alpha_z^2$.
It is important to highlight that the "default" state of a true dermal tissue is always that of state S_1. However, in our model, we describe the system using the values of the relevant variables at the reference state S_0. This is possible because we understand the process that governs the transition from S_0 to S_1 and S_2, which is precisely defined by the deformation tensors $\mathbf{F}_1$ and $\mathbf{F}_2$.
In the forthcoming derivation, we will demonstrate that the variables A_0, B_0, Z_0, and T_{res} can be determined

entirely based on their values in states S_1 and S_2 using the governing equations. The first essential component in determining the initial configurations of the model is the radial stress at the residual stressed state. To compute this, we will begin by deriving the expression for $R(R_0;t)$. To do so, we recall the fundamental assumption of morpho-elasticity, which states that $\mathbf{F}_1 = \mathbf{A}_1 \cdot \mathbf{G}_1$ for some elastic and growth tensors. However, any growth takes place in state S_1, allowing us to assume that $\mathbf{G} = \mathbf{I}$.
By substituting the values of γ_i, where $i = r, \theta, z$, with 1 in equation (1), we obtain:

$$R^2(R_0) = \frac{R_0^2}{\lambda_1} \Rightarrow R(R_0) = \frac{R_0}{\sqrt{\lambda_1}},$$

Here, λ_1 represents the axial stretch associated with the deformation described by $\mathbf{F}_1$. We can determine its value by imposing $R(B_0) = B$, which leads to $\lambda_1 = \frac{B_0^2}{B^2}$. Consequently, the expression for R can be given as:

$$R(R_0) = \frac{B}{B_0} R_0.$$

Now that we have determined R, we can express the stress components (4) explicitly in terms of R by utilizing the relationship:

$$\mathbf{F} = \operatorname{diag}\left(\frac{\partial r}{\partial R_0}, \frac{r}{R_0}, \lambda\right) = \mathbf{A} \cdot \mathbf{G} = \operatorname{diag}(\alpha_r \gamma_r, \alpha_\theta \gamma_\theta, \alpha_z \gamma_z).$$

Consequently, we obtain the following equations:

$$\begin{cases} \alpha_r = \frac{R_0}{R\lambda_1} = \frac{B_0}{B\lambda_1} = \frac{B}{B_0} \\ \alpha_\theta = \frac{R}{R_0} = \frac{B}{B_0} \\ \alpha_z = \lambda_1 = \frac{B_0^2}{B^2}. \end{cases}$$

Since $\alpha_r = \alpha_\theta$, from equation (4), we deduce that $T_{rr} = T_{\theta\theta}$, so equation (3) becomes

$$T'_{rr} = 0 \Rightarrow T_{rr} = C, \;\; C \in \mathbb{R}.$$

However, recall that in state S_1, the residual tension is due to pressure at the external boundary, that is $T_{rr}(B_0) = T_{res}$. We know then that the radial stress will be constantly equal to the residual stress in that state of the deformation. Furthermore, applying equation (4) one gets

$$T_{rr} = T_{res} = \mu\alpha_r^2 - p = \mu(\alpha^2 - \alpha_z^2) = \mu\left(\frac{B^2}{B_0^2} - \frac{B_0^4}{B^4}\right). \tag{5}$$

The next essential component is the determination of the radial stress at the recoiled state. In order to calculate this, we will employ the same approach as before. Utilizing the fundamental assumption of morpho-elasticity once again, we are aware that $\mathbf{F}_2 = \mathbf{A}_2 \cdot \mathbf{G}_2$ holds true, where $\mathbf{A}_2$ and $\mathbf{G}_2$ represent elastic and growth tensors, respectively. However, it is important to note that growth only manifests during the healing phase of the model. For our purposes, we can assume $\mathbf{G}_2 = I$, where I represents the identity tensor.
Utilizing this information, equation (1), and the fact that $r(A_0) = a_R$ at this point, we can deduce that

$$r^2(R_0, t) = a_R^2 + 2\int_{A_0}^{R_0} \frac{\bar{R}}{\lambda_2} d\bar{R} = a_R^2 + \frac{R_0^2 - A_0^2}{\lambda_2} \tag{6}$$

where λ_2 represents the axial stretch associated with the deformation defined by $\mathbf{F}_2$. We can now express the

stress components (4) in terms of r by utilizing equation (2) as follows:

$$T_{rr} = \mu \frac{R_0^2}{r^2 \lambda_2^2} - p, \quad T_{\theta\theta} = \mu \frac{r^2}{R_0^2} - p$$

Determining the radial stress is straightforward now, as we simply need to substitute these values into equation (3) and integrate. It is important to note that $T_{rr}(a_R) = 0$, as the inner surface is free of stress at the moment when the wound is created. Therefore, we have:

$$T_{rr}(r) = \int_{a_R}^{s} \frac{\partial T_{rr}}{\partial r}(s) ds = \int_{a_R}^{s} \frac{1}{s} \left(T_{\theta\theta}(s) - T_{rr}(s) \right) ds = \mu \int_{a_R}^{s} \frac{1}{s} \left(\frac{s^2}{R_0^2} - \frac{R_0^2}{s^2 \lambda_2^2} \right) ds = (*).$$

At this point, equation (6) will be useful, since

$$s^2 = a_R^2 + \frac{R_0^2 - A_0^2}{\lambda_2} \Leftrightarrow R_0^2 = \left(s^2 - a_R^2 \right) \lambda_2 + A_0^2$$

Using the latter we can continue the computation as

$$\begin{aligned}
(*) &= \mu \int_{a_R}^{s} \frac{1}{s} \left(\frac{s^2}{\left(s^2 - a_R^2 \right) \lambda_2 + A_0^2} - \frac{\left(s^2 - a_R^2 \right) \lambda_2 + A_0^2}{s^2 \lambda_2^2} \right) ds \\
&= \mu \int_{a_R}^{s} \frac{1}{\left(s^2 - a_R^2 \right) \lambda_2 + A_0^2} - \frac{1}{s \lambda_2} + \frac{a_R^2 \lambda_2 - A_0^2}{s^3 \lambda_2^2} ds \\
&= \frac{\mu}{2\lambda_2} \log \left(\left(s^2 - a_R^2 \right) \lambda_2 + A_0^2 \right) - \mu \frac{1}{\lambda_2} \log(s) \Big|_{a_R}^{r} - \frac{\mu}{2} \frac{a_R^2 \lambda_2 - A_0^2}{\lambda_2^2} \frac{1}{s^2} \Big|_{a_R}^{r} \\
&= \frac{\mu}{2\lambda_2} \left(\log \left(\frac{\left(r^2 - a_R^2 \right) \lambda_2 + A_0^2}{A_0^2} \right) - \log \left(\frac{r^2}{a_R^2} \right) + \left(\frac{A_0^2}{\lambda_2} - a_R^2 \right) \left(\frac{1}{r^2} - \frac{1}{a_R^2} \right) \right).
\end{aligned}$$

Recall that even when the skin is wounded, it is subjected to the residual stress and in consequence, it has to be satisfied that $T_{rr}(b_R) = T_{\text{res}}$. Then, we can equate (5) and $T_{rr}(b_R)$, yielding

$$\frac{1}{2\lambda_2} \left(\log \left(\frac{\left(b_R^2 - a_R^2 \right) \lambda_2 + A_0^2}{A_0^2} \right) - \log \left(\frac{b_R^2}{a_R^2} \right) + \left(\frac{A_0^2}{\lambda_2} - a_R^2 \right) \left(\frac{1}{b_R^2} - \frac{1}{a_R^2} \right) \right) + \left(\frac{B_0^4}{B^4} - \frac{B^2}{B_0 2} \right) = 0 \tag{7}$$

Finally, we also have the axial load applied to the top surface of the annuli, which can be expressed as follows:

$$N_z = \int_{a_R}^{b_R} T_{zz}(r) dr = 0 \tag{8}$$

as a consequence of the plane stress assumption. However, we can establish a relationship between T_{zz} and T_{rr} by considering that:

$$T_{zz} = \mu \alpha_z^2 - p = \mu \alpha_z^2 - \mu \alpha_r^2 + T_{rr}.$$

By substituting the derived value of T_{zz} into the equation for axial load, we obtain an additional equation that involves the variables in the initial state. Equations (5), (7), and (8) form a system of equations that can be solved to determine the values of A_0, B_0, Z_0, and T_{res}.

2 Wound modelling

2.1 Question 1

As implied by the statement of this wound modelling problem, we can exploit the symmetries inherent in the problem to greatly diminish the computational domain's size. It is worth noting that the sketch depicted in Figure (**??**) exhibits symmetry in both the horizontal and vertical directions. Consequently, the solution can be fully determined by considering only one of its "quadrants".
Therefore, we will focus on solving for the upper-left quadrant exclusively. However, in doing so, we must establish the new boundary conditions that emerge from slicing the entire domain. For the new domain:

- The top layer and the slit surface have free Neumann boundary conditions.
- The left layer has non-homogeneous Neumann conditions, equivalent to that of a uniform traction load.
- The part of the right layer which is not on the slit has null horizontal displacements, but unconstrained vertical ones.
- The bottom layer has null vertical displacements, but unconstrained horizontal ones.

Figure (2) illustrates the Finite Element Method (FEM) solution obtained considering linear elasticity for the top-left quadrant. Additionally, it includes a sketch of how the complete solution is reconstructed by appropriately reflecting the former solution:

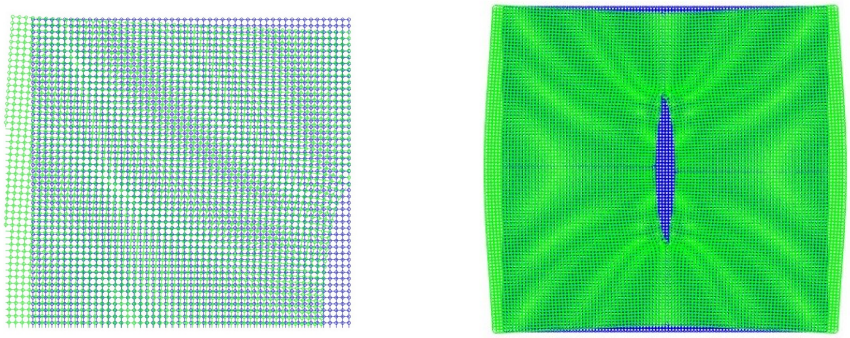

Figure 2: Original (blue) and deformed (green) FEM nodal configurations of the specimen, for both the upper-left quadrant (left) and the complete domain (right).

To create the illustrative sketch, the following material parameters were utilized: $\nu = 0.3$ (Poisson's ratio) and $E = 1$ (Young's modulus). Additionally, the magnitude of the applied traction was set at $|t| = 0.02$, and the size of the complete domain was defined as $L = 1$.

2.2 Question 2

Figure (3) depicts the plots illustrating the relationship between the maximum opening, represented by d, and the Young Modulus, denoted as E, as well as the magnitude of the traction, denoted as $|\mathbf{t}|$. In the case where E varies, we set $|\mathbf{t}|$ to a fixed value of 0.03. Conversely, when $|\mathbf{t}|$ varies, we set E to a constant value of 20.
The observed qualitative behavior in both plots aligns with intuitive expectations. Increasing the Young Modulus corresponds to an augmentation in material stiffness, resulting in a reduction in the maximum opening d.

Conversely, amplifying the magnitude of the applied lateral load, represented by $|\mathbf{t}|$, leads to an increase in the corresponding maximum opening d.
Moreover, the figure exhibits distinctive patterns that align with the linear nature of the elasticity problem being solved. As anticipated, the solutions display linearity. Consequently, we observe a linear inverse relationship between the maximum opening d and the Young Modulus E. Additionally, there is a clear linear proportionality between the maximum opening 'd' and the magnitude of the applied lateral load $|\mathbf{t}|$.
Linear elasticity leads to linear results. Let us illustrate it mathematically. The linear system is

$$\mathbf{Ku} = \mathbf{f},$$

with $\mathbf{K} \propto E$ and $\mathbf{f} \propto |\mathbf{t}|$.
Let us define the quantities in order to build the non-dimensionalization

$$\mathbf{K_E} := \frac{\mathbf{K}}{E} \quad \mathbf{f}_t := \frac{\mathbf{f}}{|\mathbf{t}|} \quad \boldsymbol{\alpha} = \frac{|\mathbf{t}|}{E}.$$

Then, substituting in the linear system we obtain

$$\mathbf{Ku} = \mathbf{f} \Rightarrow (E\mathbf{K_E})u = (|\mathbf{t}|\mathbf{f}_t) \Rightarrow \mathbf{K_E}u = \boldsymbol{\alpha}\mathbf{f}_t. \tag{9}$$

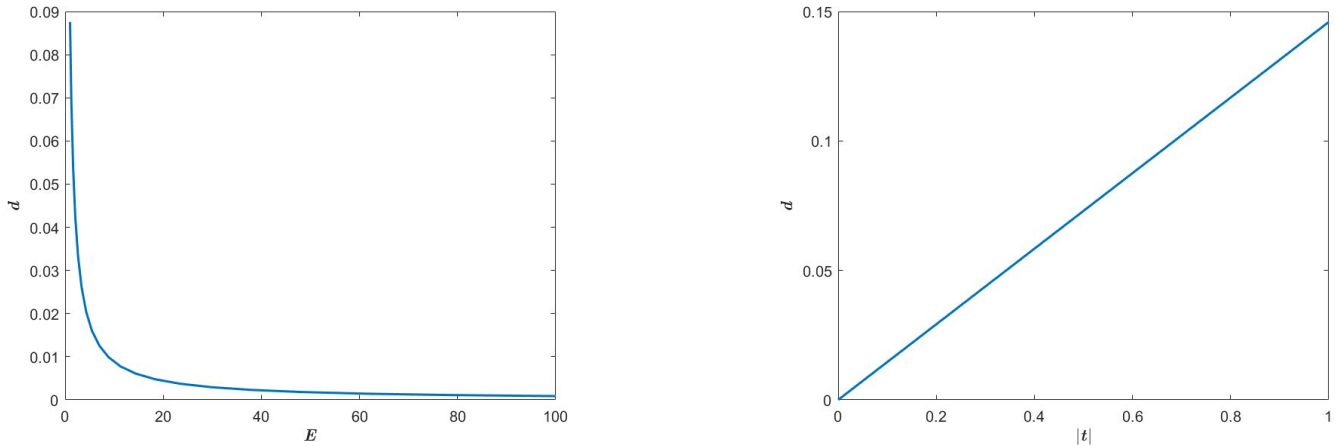

Figure 3: Comparison of maximum opening d versus Young modulus E and traction magnitude $|\mathbf{t}|$ curves.

2.3 Question 3

Figure (4) illustrates the evolution of the maximum opening d as it relates to the slit dimension l for various combinations of the Young Modulus E and the magnitude of the traction $|\mathbf{t}|$. It is evident that there exists a one-to-one mapping between d and l, similar to what was observed for the pairs d and E, as well as d and $|\mathbf{t}|$ previously. However, in those instances, either $|\mathbf{t}|$ or E was held constant, preventing the curve $d(l)$ from simultaneously determining both values. Thus, it is necessary to have at least one of them predetermined.
To support this assertion, we refer to the dashed-black and solid-yellow curves depicted in Figure (4). These curves demonstrate that different combinations of E and $|\mathbf{t}|$ can result in the same values. This phenomenon can be explained by Equation (9) which reveals that two pairs of values, $(E_1, |\mathbf{t_1}|)$ and $(E_2, |\mathbf{t_2}|)$, will yield identical outcomes as long as the ratio of $\frac{|\mathbf{t_1}|}{E_1}$ is equal to the ratio of $\frac{|\mathbf{t_2}|}{E_2}$, represented by the constant α.

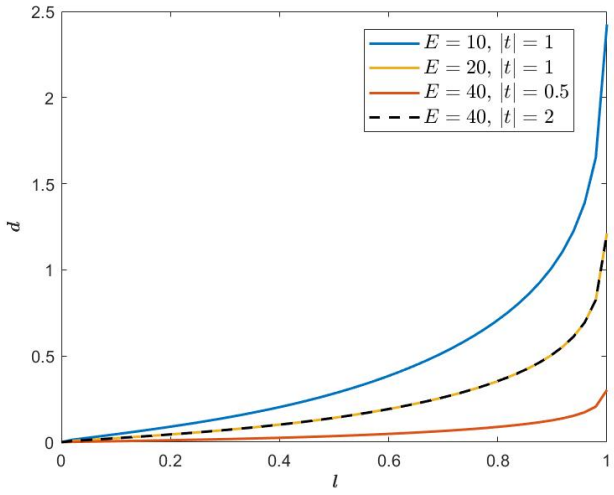

Figure 4: Maximum opening d versus slit length l for different material parameters and boundary traction.

The previous figure is also helpful in order to delve into the exploration of the problem's dependency on parameter tuning for the domain design. The boundary conditions change as a result of the varying domain configuration. An interesting effect can be observed as the parameter $l \to L$. A vertical asymptotic behavior is observed for all parameter configuration because the problem reduces to the scenario of two separate pieces of tissue being pulled apart.

The wound domain is discretized, and the level of resolution in the grid influences the continuity of the wound shape. As the grid's resolution increases, the observed shapes become smoother. For this figure, a mesh of 50×50 nodes was employed to calculate the response for an individual quarter of the wound. However, when only 20 nodes per quarter were used, the obtained response exhibited a significantly more uneven and bumpy appearance.

References

[1] Lucie Bowden, Helen Byrne, Philip Maini, and Derek Moulton. *A morphoelastic model for dermal wound closure*. In: *Biomechanics and modeling in mechanobiology* 15 (Aug. 2015). DOI: 10.1007/s10237-015-0716-7.

[2] Larry Taber. *Nonlinear Theory of Elasticity: Applications in Biomechanics*. Jan. 2004. DOI: 10.1142/9789812794222.